Journal of Biotechnology 390 (2024) 71–79

Contents lists available at ScienceDirect

Journal of Biotechnology

journal homepage: www.elsevier.com/locate/jbiotec

Cell-based shear stress sensor for bioprocessing

Taehong Kwon [a,1], Ann-Cathrin Leroux [b,1], Han Zang [c], David Pollard [a], Christoph Zehe [b], Samin Akbari [a,*]

[a] Sartorius Stedim North America Inc., United States
[b] Sartorius Stedim Cellca GmbH, Germany
[c] Boston University, Boston, MA, USA

ARTICLE INFO

Keywords:
Shear stress
Sensor
Bioprocessing
Bioreactor
CHO cell

ABSTRACT

Shear stress during bioreactor cultivation has significant impact on cell health, growth, and fate. Mammalian cells, such as T cells and stem cells, in next-generation cell therapies are especially more sensitive to shear stress present in their culture environment than bacteria. Therefore, a base knowledge about the shear stress imposed by the bioprocesses is needed to optimize the process parameters and enhance cell growth and yield. However, typical computational flow dynamics modeling or PCR-based assays have several limitations. Implementing and interpreting computational modeling often requires technical specialties and also relies on many simplifications in modeling. PCR-based assays evaluating changes in gene expression involve cumbersome sample preparation with the use of advanced lab equipment and technicians, hampering rapid and straightforward assessment of shear stress. Here, we developed a simple, cell-based shear stress sensor for measuring shear stress levels in different bioreactor types and operating conditions. We engineered a CHO-DG44 cell line to make its stress sensitive promoter EGR-1 control GFP expression. Subsequently, the stressed CHO cells were transferred into a 96 well plate, and their GFP levels (population mean fluorescence) were monitored using a cell analysis instrument (Incucyte®, Sartorius Stedim Biotech) over 24 hours. After conducting sensor characterization, which included chemical induced stress and fluid shear stress, and stability investigation, we tested the shear stress sensor in the Ambr® 250 bioreactor vessels (Sartorius Stedim Biotech) with different impeller and vessel designs. The results showed that the CHO cell-based shear stress sensors expressed higher GFP levels in response to higher shear stress magnitude or exposure time. These sensors are useful tools to assess shear stress imposed by bioreactor conditions and can facilitate the design of various bioreactor vessels with a low shear stress profile.

1. Introduction

Understanding and measuring fluid shear stress in stirred tank bioreactors is crucial in bioreactor development and process scale-up (Gareau et al., 2014; Kamen et al., 1992). Fluid shear stress results from mechanical agitation through impellers and gas bubbles arising from aeration. Its magnitude depends on many factors such as rotational speed of the impeller, geometry of the bioreactor vessel and impeller, and viscosity of cell culture. Since excessive shear stress could reduce the growth and viability of various cell lines used in bioreactor cultivation, it is important to predict and measure shear stress accurately to operate bioreactors within the stress tolerance level of cells.

The common practice to evaluate fluid shear stress is to perform computational fluid dynamics to model the flow (Ding et al., 2019; Guyot et al., 2015; Julaey et al., 2016; Verma et al., 2019). However, this computational modeling has several limitations. First, it is challenging to simulate a turbulent three-phase (air, medium, and cells) fluidic system (Julaey et al., 2016). In addition, modeling often requires many simplifications in terms of cell size, shape, concentration, culture viscosity, *etc.*, which cannot be representative of real bioreactor cultivation. Furthermore, interpretation of the results is often complicated (*e.g.*, whether to minimize average or maximum shear stress). Another approach for shear stress characterization is to use PCR methods to measure levels of gene expression of cells under shear stress (Dong et al., 2009; Gareau et al., 2014; McCormick et al., 2003; Okahara et al., 1995). Despite its robust and precise measurement, PCR-based assay has some limitations such as cumbersome sample preparation (*e.g.*, nucleic acid extraction), the varied sequential tasks spanning the entire process, and

* Correspondence to: Sartorius Stedim North America, Inc., MA 02210, USA.
E-mail address: samin.akbari@sartorius.com (S. Akbari).
[1] Taehong Kwon and Ann-Cathrin Leroux contributed equally to this work.

https://doi.org/10.1016/j.jbiotec.2024.04.016
Received 26 October 2023; Received in revised form 15 March 2024; Accepted 24 April 2024
Available online 27 April 2024

high cost (equipment, skills, reagents, *etc.*) (Petralia and Conoci, 2017). Assays assessing cell viability, morphology, and/or cell growth (Kepp et al., 2011; Stoddart, 2011) can be an alternative to detect more severe physiological disturbances caused by fluid shear stress. However, these assays are too general and do not specifically target the pathways induced by shear stress. There are various causes for changes in viability and morphology besides shear stress (*e.g.*, lack of nutrients, accumulation of toxic byproducts or lack in oxygen).

Several studies have designed cell-based stress sensors that provide a cell related, measurable response to cellular stressors (*e.g.*, nutrient deprivation, oxygen shortage, hyperosmolality or shear force) (Polizzi, 2022; Polizzi and Kontoravdi, 2015; Zeh et al., 2022). These cell-based sensors are based on stress responsive elements integrated into a promoter that controls reporter genes like fluorescent proteins or luciferase. Focusing on shear stress, one study designed HEK293 cells with shear-stress-inducible transcription factors AP1 and SP1 controlling luciferase expression (Seefried et al., 2010); The cells exhibited increased luciferase signal upon mechanical stretching. Additionally, NIH3T3 cells containing an EGR-1 promoter controlling RFP expression showed increase in RFP signal under different dispensing velocities used during fluorescence activated cell sorting (FACS) (Varma et al., 2017); this was used to optimize FACS settings towards low shear stress exposure.

To the best of our knowledge, no other studies have yet demonstrated CHO cell-based fluid shear stress sensor in bioreactors. Despite the widespread use of Chinese hamster ovary (CHO) cells for biologics production in bioreactor cultivations (Wurm and Wurm, 2021), there is an industry demand to verify shear stress levels in CHO cell processes during development and production. This is due to the potential for suboptimal culture performance caused by specific culture conditions and bioreactor setups, necessitating the identification of contributing factors to these discrepancies. By adjusting the plasmid design introduced by Varma et. al (Varma and Voldman, 2015), we developed our CHO cell-based shear stress sensor for bioreactor cultivation (Fig. 1). We selected a monoclonal CHO-DG44 cell line that expresses GFP in response to shear stress following single cell cloning protocols. The selected cell line showed the highest sensitivity to shear stress of all cell lines generated and is stable for 40 days in culture. This cell-based sensor is based on the stress sensitive promoter EGR-1 that controls GFP expression and is switched on when the cell experiences shear stress. We characterized performance of the shear stress sensor in a microfluidic channel with precise control over the flow rate and live cell imaging. The GFP expression in these cells was dependent on both shear stress magnitude and exposure time. Then, we cultured the cells in two different Ambr® 250 bioreactors with different impeller and vessel designs under various stirring speeds and culture durations. The average fluorescence intensity of the cells was dependent on stir rate, culture duration, and vessel type. Although predicting the exact shear stress value is not yet feasible with our current sensor design, they are useful tools to compare and assess the shear stress imposed by different bioreactor vessel designs and operating conditions using conventional fluorescent microscopy, which can facilitate design of vessels and impellers with low shear profile.

2. Materials and methods

2.1. Sensor fabrication

A CHO-DG44 clone expressing IgG_1 antibody was transfected with a plasmid carrying the stress inducible EGR-1 promoter with GFP as a reporter molecule (Fig. 2). The EGR-1 promoter has been previously described to be shear stress sensitive: a panel of promoters was screened for shear stress response in NIH3T3 cells and the EGR-1 promoter showed the highest response to shear stress exposition (Varma and Voldman, 2015). In order to mimic shear stress, a chemical compound (Phorbol 12-myristate 13-acetate, PMA) was used to activate the PKC-MAPK-ERK pathway, which is part of the shear stress response (Varma and Voldman, 2015). Stable cell pools overexpressing GFP under EGR-1 control were generated by neomycin selection (Fig. 2). PMA (Sigma, P1585–1MG) was used to mimic short-term fluid shear stress because of its upregulation of EGR-1 (Varma and Voldman, 2015). PMA at a concentration of 100 nM was added to the stable EGR1-controlled GFP expressing cells and GFP fluorescence was measured 18 h post induction using flow cytometry (IqueScreener iQue® 3, Sartorius). The pool with the largest shift in GFP fluorescence was used for single cell cloning via FACS (BD FACS Aria Fusion, BD biosciences). 120 clones were screened for PMA stress responsiveness and the top 4 clones were selected. The top 4 clones were passaged every 3 days for 35 days in 125 mL shake flasks (36.8°C, 7.5 % CO_2).

2.2. Cell culture in shake flasks and stability study

CHO-DG44 cells expressing GFP under control of stress-inducible EGR-1 were cultured in medium composed of 4Cell® XtraCHO Stock & Adaptation Medium (SAM) (Sartorius, Germany), 6 mM L-glutamine (Corning, NY, USA), 15 nM methotrexate (Pfizer Pharma, PZN-3362608) and 250 µg/mL G418 (Gibco, 10131027). The CHO cells were cultivated by a standard method. Briefly, 1×10^7 cells were dispersed in 50 mL medium to achieve an inoculation concentration of 2×10^5 cells/mL in a 250 mL shake flask (4115–0250, Erlenmeyer flask,

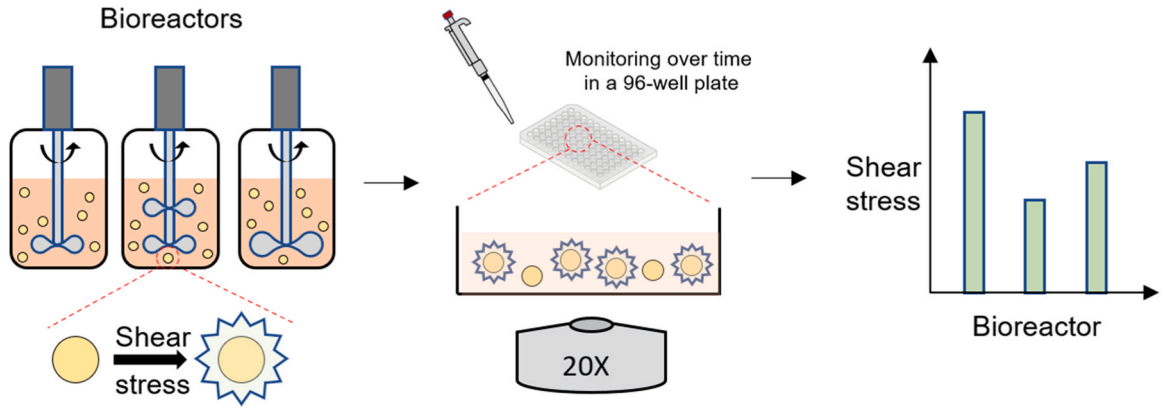

Fig. 1. Concept of measuring shear stress generated in different bioreactors using shear stress-sensitive CHO cells. The sensor CHO cells are cultured in bioreactors with different designs and operating conditions. These cells are shear stress-sensitive and emit fluorescence according to shear stress levels. A cell imaging instrument observes and analyzes fluorescence of the sampled cells over time. This study utilized fluorescence data from a 96 well plate at the 24-hour mark. Following analysis, we assess levels of shear stress in the bioreactors.

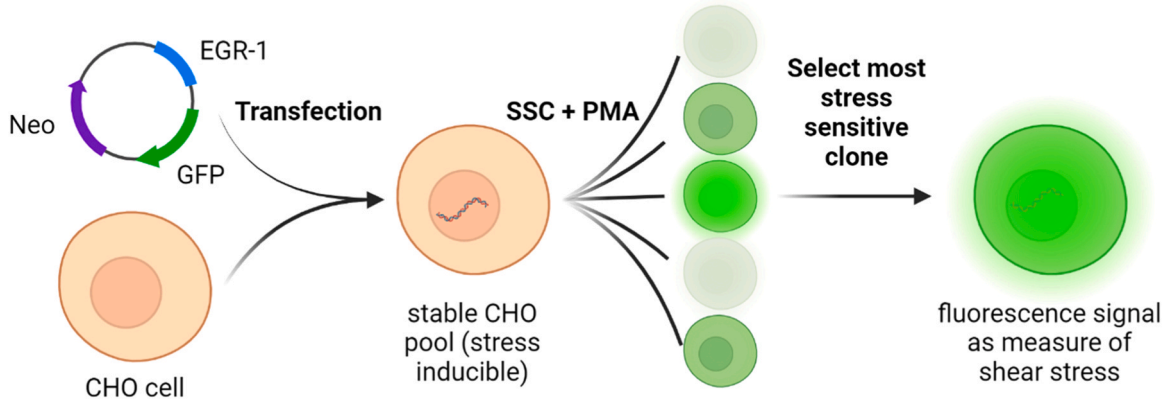

Fig. 2. Generation of stress sensitive CHO cell line. A plasmid coding for GFP under the control of the shear stress inducible promoter EGR-1 was transfected into CHO DG44 cells. Stable pools were generated by Neomycin selection. The pool with the highest shift from non-fluorescent to fluorescent state (inducibility) was selected for single cell cloning (SSC). GFP expression was induced in single cell clones by addition of PMA. The clone with the highest inducibility was selected as a new stress sensor cell line. Created with BioRender.com.

Thermo Scientific). The cells were incubated at 36.8 °C, 7.5 % CO_2 with orbital shaking at 103 rpm and passaged every 3 days. For the stability study, the cells were cultivated on a linear shaker at 110 rpm.

2.3. Sensor characterization – chemical (PMA) induced stress

Chemical-induced stress was studied using PMA (Sigma, P1585–1MG) and measured by Incucyte® (Sartorius) and flow cytometer (CytoFLEX, Beckman Coulter; iQue 3, Sartorius). PMA was dissolved in DMSO to make a stock solution of 0.5 mg/mL. For Incucyte® measurements, cells (1×10^4 cells/well) were seeded in a 96 well plate (Corning). PMA was added after 3 h of seeding to achieve final concentration of 0, 10, 100, 250, and 500 ng/mL in the wells. Upon addition of PMA, the plate was scanned with 4 images per well under GFP mode with a 10× objective every 1 h for 3 days. Exposure time was set to be 100 ms. Mean GFP fluorescent intensity of each cell were obtained by integrated GFP intensity normalization by cell area per image. For flow cytometer measurements, cells (2×10^5 cells/well) were seeded in a 24 well plate. Cell concentration reached 5×10^5 cells/mL after 3 days of cultivation. PMA was added subsequently to achieve final concentrations of 0, 10, 100, 250, and 500 ng/mL in the wells. After 24 h, cells were collected by centrifugation (190 g, 3 min), washed 3 times with PBS, and dispersed in PBS to measure GFP intensity by flow cytometry. For sensor characterization during stability assessment, 200 µL of a 2-day old culture was transferred to a 96-well plate and incubated with 100 nM PMA at 36.8°C and 7.5 % CO_2. After 17–18 h, GFP intensity was measured by flow cytometry (iQue 3, Sartorius) directly on the incubated 96-well plate.

2.4. Sensor characterization in microfluidic channels - fluid shear stress

Commercial microfluidic chips (µ-Slide VI 0.4, 80604, ibidi; height 400 µm, width 3.8 mm, length 17 mm) were used to apply fluidic shear stress to the CHO cells. The channel surface had poly-L-Lysine for cell attachment. 30 µL of CHO cells at 0.75×10^6 cells/mL were seeded to the microfluidic channel and incubated in the 7.5 % CO_2 incubator for 60 min for cell attachment. Subsequently, the tubes from the medium reservoirs were connected to the microfluidic channel through Luer-lock connection in a sterile manner. Then, the pressure pump (PG-MFC-8CH, PreciGenome) gave an oscillatory flow to the microfluidic channel at a target flow rate; the flow rate was controlled by varying pressures. The fluidic shear stress on the cells in the channel was calculated according to the following equation (ibidi GmbH, 2022):

$$\tau = \eta \bullet 176.1 \bullet \Phi$$

with τ shear stress (dyn/cm^2), η dynamic viscosity (dyn·s/cm^2), and Φ flow rate (mL/min). The dynamic viscosity of culture medium was assumed to have 0.0068 dyn·s/cm^2 (water at 37°C). Following shear stress application at different magnitudes (0, 8.0, 12.9, and 21.9 dyn/cm^2) and duration (10, 30, and 60 min), the culture medium reservoirs were disconnected from the microfluidic chip. The microfluidic chips were then placed on a tray in a live cell imaging and analysis instrument (Incucyte®, Sartorius) in a 7.5 % CO_2 incubator. The instrument captured phase contrast and fluorescent images at a regular time interval (60 min) and analyzed them automatically (cell identification and signal intensity quantification). For quantification of cellular shear-stress response, the green fluorescence signals of the cells at 24 hours after shear stress application was averaged and normalized by the fluorescence of the cells in the no-flow (*i.e.*, no shear stress) channels.

2.5. Sensor test in Ambr® 250 bioreactors

Two different types of commercial bioreactors (Ambr® 250, Sartorius) were tested: vessel A (001–2A23, baffled vessel, two pitched blade impellers, 26 mm impeller diameter) and vessel B (001–2A33, unbaffled vessel, one pitched blade impeller, 30 mm impeller size). The power number of the impeller for two vessels was 1.34 and 2.07, respectively (Sartorius Stedim Biotech, 2020). Other culture flasks (4115–0250, Erlenmeyer flask, Thermo Scientific; 658195, Suspension culture flask, Greiner) were used as low-shear reference conditions. The sensor CHO cells were cultured in shake flasks in a 7.5 % CO2 incubator on a batch mode (see Cell culture section above). After a 3-day cultivation, the cells were inoculated into Ambr® bioreactors at 0.3×10^6 cells/mL (viability: >98 %). The working volume of the bioreactor was 120–165 mL. The bioreactor medium consisted of 4Cell® XtraCHO Stock & Adaptation Medium (SAM) (Sartorius, Germany), 4Cell® XtraCHO Feed medium A and B (Sartorius, Germany), L-glutamine (6 mM), MTX (15 nM), and G418 (250 µg/mL). Antifoam C (2 v/v %; A8011, MilliporeSigma) and glucose (400 g/L; 97062–946, VWR) were prepared in separate reservoirs. The pH and DO were set to 7.1 and 60 % air saturation, respectively. They were automatically controlled by an Ambr® station (Ambr® 250 modular, Sartorius) via gassing (O_2, N_2, and CO_2). Temperature was set to 36.8 °C. Different agitation rpms (1000, 1500, 2000, and 2500) were applied to the bioreactors. The agitation power per unit volume (P/V, W/m^3) was calculated as follows:

$$\frac{P}{V} = \frac{(N_p \times \rho \times N^3 \times D^5)}{V}$$

with N_p impeller power number, ρ fluid density (kg/m^3; 1000 for water), N agitator speed (rps), D impeller outer diameter (m), and V the

bioreactor's working volume (m^3). The P/V levels for vessel A and B in this study range from 447 to 6980 and from 1411 to 11291, respectively. It is worth noting that the typical P/V level for CHO cell cultivation in vessel A falls within the range of 230–279 (at 855 rpm and with a working volume of 165–200 mL). The other flasks used as low-shear reference conditions were positioned on a shaker (Dura-Shaker, VWR) and agitated at 108 rpm. The culture samples from the Ambr® 250 bioreactors and the low-shear reference flasks were collected at different time points (0 h, 4 h, 1 day, 3 days, and 5 days). After cell concentration was counted by the automated cell culture analyzer (Cedex HiRes Analyzer, Roche), the sampled cells were seeded into the 96 well plate at 0.04×10^6 cells/mL concentration (volume: 150 µL). Subsequently, the plate was placed in the Incucyte® in the incubator (36.8°C, 7.5 % CO_2), and fluorescent shear response of the cells was automatically monitored at a regular time interval (60 min). For quantification of cellular shear response, the fluorescence signal at 24 h after seeding was used. The mean fluorescence intensity of the cells sampled from the bioreactors was normalized by the intensity of the cells from the low-shear reference flasks. Since the maximum fluorescence signal was measured 10 hours after PMA exposure and remained consistent between 10 and 24 hours after PMA induction (Fig. 5A), we chose to establish a fixed measurement time at 24 hours to enhance data comparability across different experimental runs. It is worth noting that certain bioreactor conditions (*e.g.*, those involving a 3-day exposure) exceeded the 24-hour cultivation period for sensor cells. Nevertheless, we intentionally maintained a fixed fluorescent measurement time at 24 hours after sampling to facilitate comparisons between various culture durations.

3. Results

3.1. Sensor fabrication

We generated stable CHO cell pools (LPs) that express GFP under the control of the EGR-1 promoter (stress inducible) and SV40 promoter (constitutive) (Fig. 3, Supplementary Fig. S1). Upon PMA induction, fluorescence intensity increased about 2-fold. We used the pools with the highest dynamic range upon PMA stress induction (black bars in Fig. 3) for the generation of 120 single cell clones to identify clones with higher dynamic range in stress responsiveness compared to their host pools.

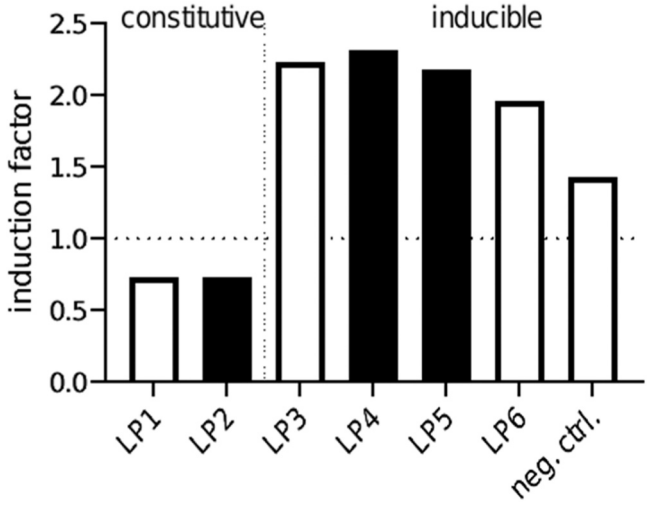

Fig. 3. Induction factor for stable pools 14 days post transfection. Inducibility of cell pools stably overexpressing GFP under control of EGR-1 promoter (inducible, LP3–6) and SF40 promoter (constitutive, LP1–2). Pools were induced with 100 nM PMA. GFP fluorescence was measured at 18 h post transfection. Black bars indicate pools that were used to generate clonal cell lines. Data was normalized to GFP fluorescence of uninduced pools.

3.2. Sensor characterization – stability test

Stability of shear stress inducibility of the cell line is critical for assessment of shear stress in a bioprocess environment. We tested the top three shear-stress-inducible clones for stability of stress inducibility. We cultivated three clonal cell lines stably expressing GFP under the EGR1-promoter (stress inducible) and one clonal cell line expressing GFP constitutively (non-inducible) over 35 days in batch culture. We induced GFP expression with PMA every three days in a separate cultivation dish. The induction factor indicates the fold change increase of GFP fluorescence intensity with *vs*. without PMA induction (Fig. 4). Generally, there is a fluctuation of the induction factor visible over time. The clones showed a similar average stress inducibility compared to their host pools. Since clone 69 showed the highest PMA inducibility over time, we chose this clone for the shear stress evaluation of different Ambr® 250 bioreactor vessels.

3.3. Sensor characterization – PMA induced stress

PMA is known for upregulating EGR-1 and used to mimic short-term fluid shear stress (Varma and Voldman, 2015). The live cell imaging instrument (Incucyte®, Sartorius) measured GFP fluorescence of the sensor CHO cells after PMA treatment, as shown in Fig. 5. The control (PMA at 0 ng/mL), where no PMA was added, only exhibited basal GFP fluorescence intensity throughout the entire recording period (72 h). PMA at 10 ng/mL induced lower level of increased GFP fluorescence intensity compared with 100, 250, and 500 ng/mL PMA. GFP fluorescence intensity increased and plateaued in the first 10 h and decreased from 24 h after PMA addition. The fold change in GFP fluorescence intensity of the exposed cells, normalized to the fluorescence intensity of the control cells where no PMA was added (0 ng/mL PMA) at 24 h, was 2.32-fold, 2.46-fold, 2.47-fold, and 2.61-fold for 10, 100, 250, and 500 ng/mL PMA, respectively. The flow cytometer measured the percentage of activated cells, which was found to be 2.8 %, 27.5 %, 53.9 %, 57.1 %, and 58.1 % for the control, 10, 100, 250, and 500 ng/mL PMA, respectively (Supplementary Fig. S2).

3.4. Sensor characterization – fluid shear stress

We used the microfluidic channels and Incucyte® to characterize the fluidic shear response of the sensor CHO cells (Fig. 6A and Supplementary Fig. S3). The microfluidic channels allowed the cells to be under oscillatory flow at different shear magnitudes and durations while Incucyte® monitored the GFP expression by the cells under shear stress. Fig. 6B shows the shear stress response at different magnitudes (8.0, 12.9, and 21.0 dyn/cm^2) at a fixed duration (30 min). The fluorescence

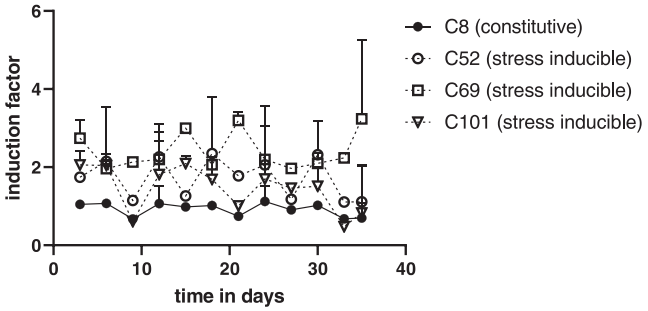

Fig. 4. Stability assessment of stress inducible CHO cell lines. Inducibility of generated stress inducible clones over a cultivation period of 35 days. Cells were treated after two days of cultivation with 100 nM PMA. GFP fluorescence intensity was measured after an incubation period of 17–18 hours by flow cytometry (iQue® 3, Sartorius). Each symbol represents the average of two measurements of the same cell culture (error bars indicate the standard deviation).

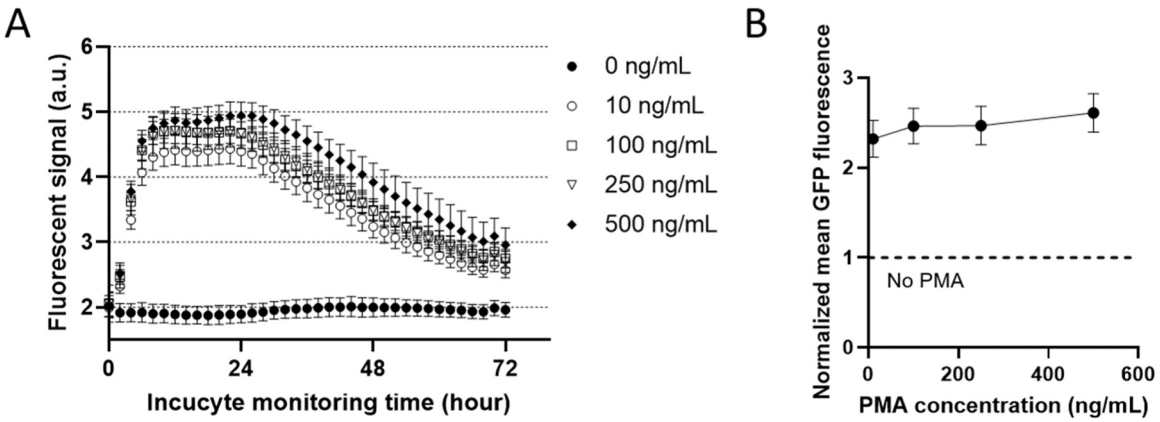

Fig. 5. GFP fluorescent responses of the cells under chemical induction using PMA at different concentrations. PMA was added at 0 hours, and the fluorescence intensity of individual cells was measured using Incucyte®, a live cell imaging and analysis instrument from Sartorius. (A) Fluorescent signal over the monitoring period. The error bars represent the standard deviation of eight technical replicates, which correspond to the same cell culture in separate microwells. (B) Normalized GFP fluorescence at different PMA concentrations at 24 hours (No PMA = 1, data from Fig. 5A).

levels of the cells at low shear stress (8.0 and 12.9 dyn/cm^2) were similar to the no-flow (*i.e.*, no shear stress) control. However, with a further increase in stress magnitude to 21.0 dyn/cm^2 there was a higher fluorescence level. The increase in mean fluorescence was 6 %.

In addition to stress magnitude, we tested different durations (10, 30, and 60 min) of shear stress (Fig. 6C). The shear stress level was fixed at 21.0 dyn/cm^2. Compared to the cells in no-shear-stress channels, the normalized shear stress levels for three different durations were 0.98, 1.06, and 1.23, respectively. The longer duration of shear stress application caused more fluorescent responses from the cells.

3.5. Sensor test in Ambr® bioreactors

We tested the shear response of the sensor CHO cells in a commercial small-scale bioreactor ("vessel A", power number 1.34, baffled, two impellers, impeller outer diameter 26 mm) under different shear stress conditions (Supplementary Fig. S4). Although the shear stress is not homogenous in the bioreactor setting, the average fluorescence response of the sensor cells can be representative of the shear stress magnitude and time sensed by the cells. Varying stirring speeds led to different power densities (power per unit volume; P/V in W/m^3). We tested four power densities (447, 1508, 3574, and 6980 W/m^3) at different culture durations (0 h, 4 h, 1 day, 3 days, and 5 days), as shown in Fig. 7 and Supplementary Fig. S5. The power densities of 447 and 1508 W/m^3 did not increase shear stress response regardless of culture duration. However, we observed the increase in GFP expression starting 3574 W/m^3 and after 1-day cultivation. The higher power density (6980 W/m^3) produced more shear response of the cells.

Comparison of shear stress levels in different bioreactors is possible using the cell-based shear stress sensor. The cells were cultured in another bioreactor vessel with different impellers ("Vessel B", power number 2.07, unbaffled, one impeller, impeller outer diameter 30 mm) (Supplementary Fig. S6). Fig. 8 shows the cellular response in two different bioreactors (vessel A and B) at different power densities and culture durations. Different bioreactor conditions and impeller structure produced different power densities. Compared to 0 h, both vessel A and B bioreactors during 1-day cultivation exhibited the increase in shear stress response at higher P/V. Vessel A bioreactor had 1.5 response at 3574 P/V; Vessel B bioreactor had 1.33 response at 6550 P/V. Higher signal intensity (1.89) of vessel A than vessel B (1.33) in a similar P/V range (6550–6980 W/m^3) indicates vessel A caused more shear stress on the cells than vessel B. 3-day cultivation further supports this. At a similar P/V (6550–6980 W/m^3), vessel B had smaller shear stress response than vessel A (2.62-fold difference). As P/V increased further above 10 kW/m^3, the vessel B bioreactor showed a similar high shear stress response to vessel A at 1-day and 3-day cultivation, indicating that cultivation in two bioreactors at this intense agitation condition is not suitable for cell cultivation.

4. Discussion

The current study demonstrates the cell-based shear stress sensor for bioreactor cultivation. Based on previous work showing that EGR-1 promoter is shear stress-sensitive (Varma and Voldman, 2015), we developed a CHO-DG44 clone containing shear stress-inducible EGR-1 promoter and GFP. We studied its sensitivity and stability using chemical induction and fluid shear stress. Finally, demonstration of this cell-based sensor in the actual Ambr® 250 bioreactor showed that it could assess shear stress imposed by different bioreactors and operating conditions.

We developed a stable CHO cell line with GFP expression under the control of stress inducible EGR-1 promoter. The GFP reporter gene expression of PMA-induced cells exhibited about 2- to 2.5-fold increase, compared to uninduced cells. This is comparable to the stress inducible NIH3T3 cell line created by Varma *et al.* with an 2.14 fold increase upon PMA induction (Varma et al., 2017; Varma and Voldman, 2015). We showed that the sensor response peaked at 17–24 hours post PMA induction followed by a 48-hour phase of GFP fluorescence signal reduction to levels comparable to baseline. This induction dynamics does not allow for real-time monitoring of shear stress but rather comparing different shear stress expositions (*e.g.*, different culture vessels or stirring speeds). Additionally, the dynamic range of 2-fold induction only gives a small resolution for shear stress and the stress level needed to induce GFP expression is quite high. To improve response dynamics, it would be necessary to a) decrease time from stress signal to response signal, and b) speed up reporter degradation. For example, instead of a reporter protein, a reporter siRNA could be used. This binds to a constitutively expressed fluorescent protein with short turnover times. In this case, decreasing fluorescence intensity would imply an increase in shear stress. This siRNA approach could reduce response time, as protein expression is bypassed. To increase sensitivity, it may be possible to consider alternative cell types that are more susceptible to shear stress than CHO cells and might exhibit EGR-1 promoter activation at lower shear stress levels. Alternatively, it may be possible to explore or identify other shear stress-sensitive promoters. For instance, when considering alternative cell types, Induced Pluripotent Stem Cells (iPSCs) could serve as more sensitive reporter cells. They are well-known for their shear sensitivity and are comparatively more fragile than CHO cells (Bender, 2021). Given the increasing importance of novel modalities such as stem cells in today's bioprocessing landscape, where bioreactor operation

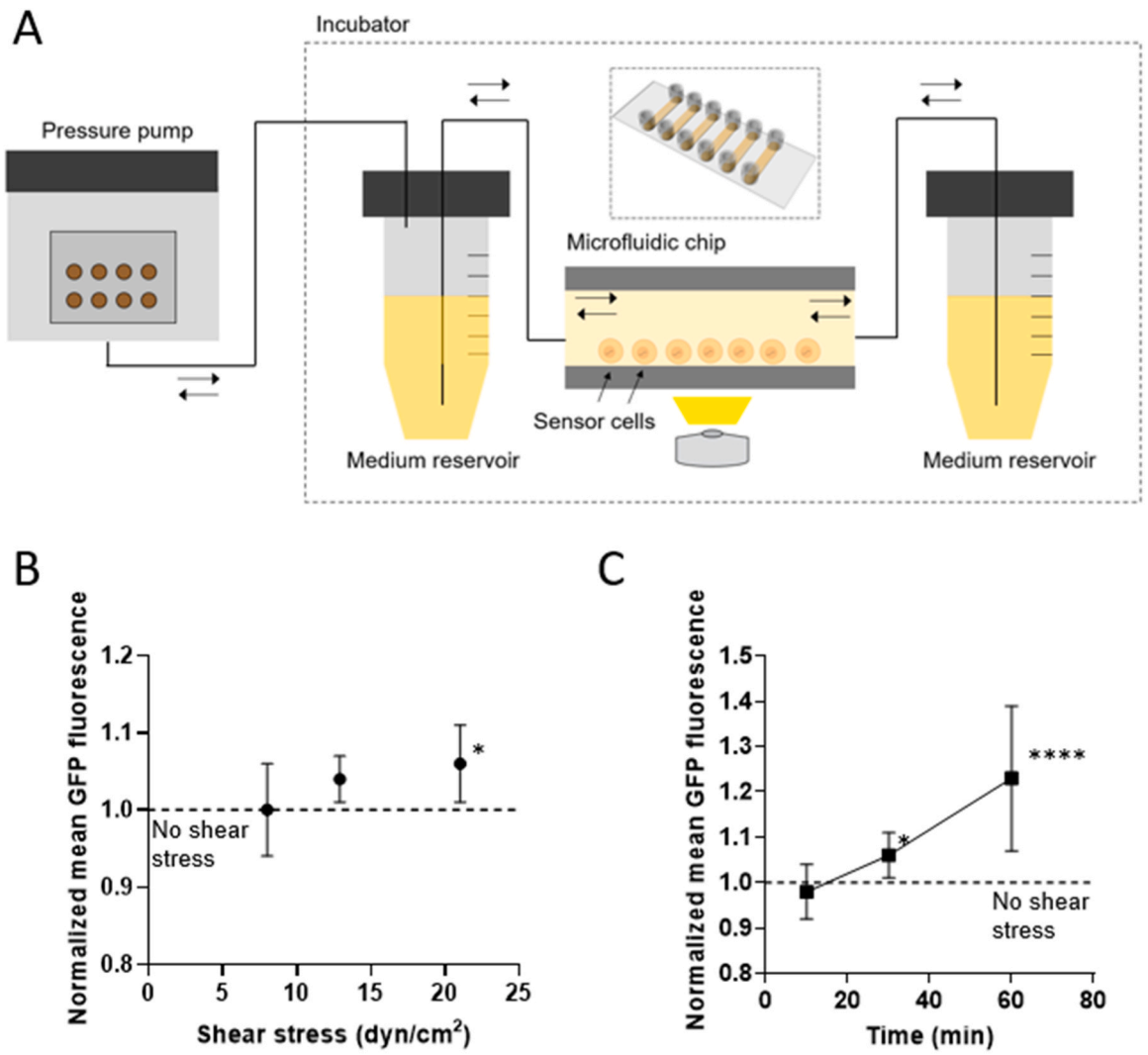

Fig. 6. The setup for applying fluid shear stress to the sensor CHO cells and shear stress response of the cells at various magnitudes and durations. The data presented in this figure was derived from microfluidic experiments measuring fluorescence intensity 24 hours after the application of shear stress. The response was normalized relative to the absence of shear stress. Error bars represent the standard deviation across three independent experiments. For statistical analysis, Student's t-test was employed. Asterisks (*) were used to denote the level of statistical significance (*: $p<0.05$, ****: $p<0.0001$) when compared to the no-shear-stress condition. (A) The setup for applying fluid shear stress to the cells. The cells were attached to the Poly-L-Lysine (PLL)-coated surface within a commercial microfluidic chip (μ-Slide VI 0.4, ibidi) and exposed to oscillatory fluid flow generated by a programmed pressure pump (PG-MFC-8CH, PreciGenome). The images were captured using Incucyte®. (B) GFP fluorescence response of the cells at different shear stress magnitudes (duration fixed at 30 min). The no-shear-stress condition exhibited an average value of 1.0 ± 0.04 (average ± standard deviation, $n = 18$). (C) Response at various durations of shear stress (shear stress fixed at 21.0 dyn/cm^2). The no-shear-stress condition showed an average value of 1.0 ± 0.03 (average ± standard deviation, $n = 16$).

plays a critical role in mass production for clinical and commercial purposes, monitoring shear stress using iPSCs has the potential to enhance bioreactor design and optimize its operation.

It is conceivable that our CHO cell-based sensor could respond to alternative stressors that stimulate EGR-1 transcription or its upstream events in a manner similar to fluidic shear stress. Varma and Voldman highlighted a constraint in the specificity of transcriptional sensors that depend on a single node within biological pathways (Varma and Voldman, 2015). Many genes responsive to shear forces (*e.g.*, EGR-1, c-fos, KLF2) are activated downstream of MAP kinase signaling (Traub and Berk, 1998; Young et al., 2009). Therefore, any activators that engage common upstream pathways, including inflammatory cytokines and reactive oxygen species, might also induce the expression of shear-responsive genes through these shared pathways. We initially explored the effect of oxygen deprivation on these cells, which did not result in a measurable GFP expression. In this study, we have focused on using our sensors in situations where the sole variable stimulus is fluidic shear stress (*e.g.*, excluding conditions involving starvation or low oxygen levels). However, it is worth noting that a more sensitive sensor might respond to oxygen or nutrient deprivation.

We employed overall GFP fluorescence (population mean fluorescence) as our metric to represent stress, similar to the approach used in Varma and Voldman's work (Varma and Voldman, 2015). We made this choice due to the relatively small portion of activated cells (approximately 1.5-fold increase) and the high dynamic range observed (around 2.5-fold upon induction). The variation in GFP production among cells can be attributed to several factors, including non-uniform gene insertion, non-uniform shear stress in the chamber (resulting in cells experiencing different shear stress levels), and the non-uniform cell population, a well-known characteristic of CHO cell culture (Davies et al., 2013). For example, not all CHO cells produce the same amount of antibodies in the bioreactor. Controlling all of these aforementioned factors is currently not feasible. Therefore, it is worth noting that our averaging method, which considers a small proportion of activated cells,

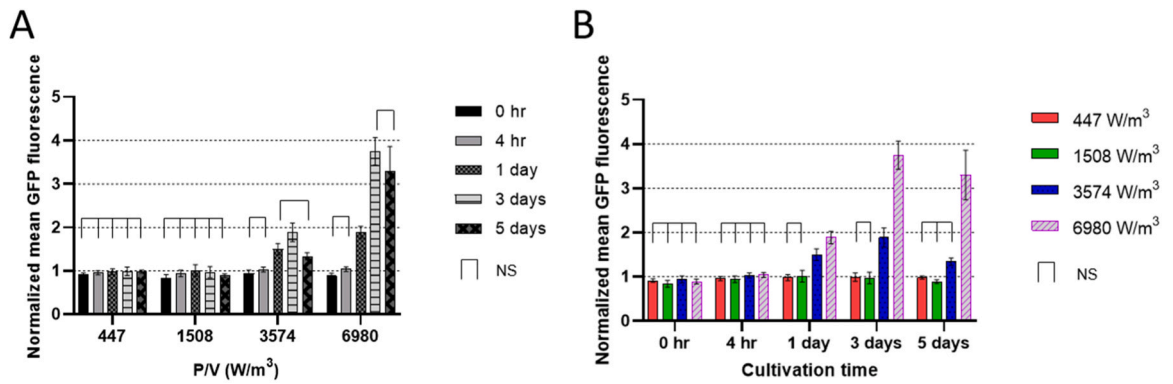

Fig. 7. Shear stress response of the cells in a commercial small-scale bioreactor (Type A) at various power densities and cultivation times. Stirring speed was adjusted to vary power density, and fluorescence was normalized using low-shear reference culture flasks ($n = 2$) placed on a shaker. The data in this figure were derived from five technical replicates, with a coefficient of variance (CV) for these replicates of 4.5 % ± 3.9 %. Error bars represent standard deviations. For statistical analysis, an ordinary one-way ANOVA with Tukey's multiple comparisons test (significant level of 0.5) was employed. "NS" in the figure denotes "not significant." Detailed statistical analysis results can be found in Table S3 and S4. (A) Power density (x axis) *vs.* shear stress response (y axis) plot. (B) Cultivation time (x axis) *vs.* shear stress response (y axis) plot.

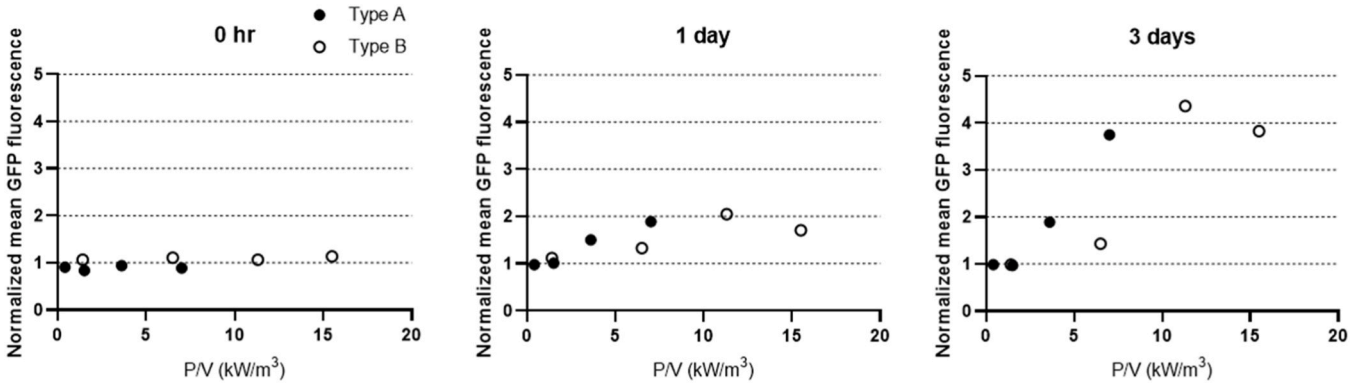

Fig. 8. Cellular shear stress responses in two different bioreactors (Type A and B) at different power densities and culture durations. Fluorescence was normalized by low-shear reference culture flasks ($n = 2$) placed on a shaker. The average of 5 technical replicates was used for each condition. The values in this figure were obtained from five technical replicates, and the coefficient of variance (CV) for these replicates was 6.0 % ± 4.2 %.

has certain limitations. Under conditions of intense shear stress, there may potentially be both higher GFP production per cell and an increased proportion of activated cells. Nevertheless, our current metric, based on population mean fluorescence, may not fully capture these specific details. Additionally, as cells move around and experience both high shear and low shear zones, our method is unable to distinguish between regions with varying shear conditions in bioreactor cultivation. This differentiation can be achieved through computational fluid dynamics modeling. Despite these limitations, the benefit of our cell-based shear sensor lies in its ability to measure the overall stress that the cell population experiences and provide a real-life metrics for determining whether it falls within acceptable or detrimental ranges.

We used flows in the microfluidic channels to characterize the sensitivity and operating range of the sensors before the test in bioreactors. Compared to the previous NIH3T3 cell-based shear stress sensors whose minimum detectable shear stress was 2 dyn/cm^2 for 30 minutes duration (Varma and Voldman, 2015), the current CHO cell-based sensor exhibited a lower sensitivity of 21.0 dyn/cm^2, with three tested magnitudes: 8.0, 12.9, and 21.0 dyn/cm^2. Several factors including the cell types, cell engineering methods, and microfluidic flow conditions (*e.g.*, continuous unidirectional *vs.* bi-directional) could cause this difference. Also, the maximum shear stress and duration tested in the microfluidic experiments were 21.0 dyn/cm^2 and 60 minutes, respectively, (Fig. 6). Considering higher fluorescence intensity of the sensors from the bioreactor experiments at harsh agitation conditions (Fig. 7), the sensors could detect higher magnitude and longer duration of shear stress. Testing these conditions in the microfluidic channel was challenging in the current study because of cell detachment from the channel surface at these intense shear conditions. Further optimization of bonding conditions (*e.g.*, different coating materials and conditions) could enable testing of intense fluid conditions in the microfluidic channel and make it a useful tool for shear stress calibration.

We used commercial PLL-coated microfluidic chips (ibidi) to attach the sensor cells and investigate their shear stress response at designated stress intensities (8.0, 12,9, 21.0 dyn/cm^2) and durations (10, 30, 60 min) (Fig. 6). These chips function as parallel-plate flow chambers, a commonly used setup for shear stress tests on cells (Fallon et al., 2022; Jackson et al., 2023). Notably, we observed an increase in shear stress response from the sensor cells at 21.0 dyn/cm^2 for 30 min and 60 min. Regarding the comparison to existing studies, we found numerous publications exploring the effect of shear stress on cells attached to surfaces. Many of these studies utilized parallel-plate flow chambers (Fallon et al., 2022; Jackson et al., 2023), testing various cell types, including CHO cells (Shiragami and Unno, 1994), endothelial cells (Chiu et al., 2003; Xiao et al., 2011; Zhang et al., 2019), and stem cells (Huang et al., 2019; Nsiah et al., 2014). The tested shear stress intensities were typically below 70 dyn/cm^2, aligning with *in vivo* fluid flow conditions (Riehl et al., 2017). Although the tested shear stress intensities did not result in apparent physical damage, they prompted alterations in cellular morphology, permeability, gene expression, and diverse

biochemical and physiological responses, as evidenced in earlier studies. For instance, Shiragami and Unno investigated CHO cells in a setup with two parallel flat rectangular plates and observed an increase in lactate dehydrogenase (LDH) activity over intensities (3–7 dyn/cm^2) and exposure times (1 h – 16 h) (Shiragami and Unno, 1994). Similarly, Zhang et al. demonstrated morphological changes in human umbilical vein endothelial cells at 8.4 dynes/cm^2 for 60 min (Zhang et al., 2019). Chiu and et al. observed that exposure to shear stress at 12 dyne/cm^2 for a duration of 6 hours suppressed the expression of adhesion molecules in vascular endothelial cells when co-cultured with smooth muscle cells (Chiu et al., 2003). Furthermore, significant increases in nitric oxide secretion from endothelial progenitor cells were observed at 15 dyn/cm^2 up to 24 hours (Xiao et al., 2011). Active research on the effect of shear stress on stem cell differentiation is ongoing (Huang et al., 2021). Huang et al. reported that a stress amplitude of 10 dyne/cm^2 promoted the differentiation of mouse iPSCs towards arterial endothelial cells (Huang et al., 2019), while Nsiah et al. found that pre-conditioning embryonic stem cell monolayers at 5 dyn/cm^2 promoted endothelial gene expression (Nsiah et al., 2014).

We evaluated the shear stress levels of two different Ambr® 250 vessels (type A and B) using the sensors. Both vessels exhibited higher shear stress levels at higher power density and longer duration (Fig. 8). However, type A had a steeper power density-sensor response curve than type B, indicating type A has a higher shear stress level given the similar power density. In fact, type B is a Sartorius' new Ambr® 250 bioreactor that is unbaffled and has a single elephant ear-shaped impeller (Rotondi et al., 2021). Its unique configuration provided more gentle mixing for T cells and human mesenchymal stem cells on beads and microcarriers than the baffled and double-impeller bioreactor (as in Type A), thus improving cell production (Rotondi et al., 2021). Although the sensor reported high shear stress level at intense power densities (tested up to 6980 W/m^3 for Type A and 15,525 W/m^3 for Type B; corresponding to 2000 stirring rpm), it is noted that the normal operating power densities are significantly lower than these shear response-triggering power densities. For example, 855 rpm giving 279 W/m^3 is commonly used for regular CHO cell cultivation using Type A vessel without causing shear stress. As a future work, it could be possible to test more bioreactors with different configurations.

Review articles (Chalmers, 2015; Hu et al., 2011; Pörtner et al., 2024) provide a comprehensive overview of the P/V (power density or energy dissipation rate) ranges in bioreactors that elicit non-lethal physiological responses, such as changes in membrane integrity, glycosylation, protein production, or, as observed in this study, alterations in gene expression. According to the latest review (Pörtner et al., 2024), the observed P/V ranges of non-lethal and lethal responses were approximately 600–6000 W/m^3 and >30,000 W/m^3, respectively. Considering the P/V levels in our study (vessel A: 447 – 6980 W/m^3, vessel B 1411 to 11,291 W/m^3), all except the lowest value (447 W/m^3) fall within the range associated with sub-lethal responses (Fig. 7 and Supplementary Fig. S6). Notably, conditions with P/V values of 3574 W/m^3 or higher for vessel A and 6550 W/m^3 or higher for vessel B exhibited an increase in shear stress response (shear stress-related gene expression) over cultivation period. However, we acknowledge that moderately low P/Vs, such as 1508 W/m^3 for vessel A, did not induce an increase in shear stress response, although falling within the range associated with a non-lethal response. It is crucial to recognize that other non-lethal responses, not explored in our study (*e.g.*, glycosylation or productivity changes), could occur. Given the ongoing gaps in understanding the connection between hydrodynamics and biological processes, especially in the context of process design, additional research that establishes links between hydrodynamics and cellular effects is essential for enhancing our process understanding (Pörtner et al., 2024). A judicious integration of experimental and model-based (CFD) approaches holds promise in addressing this challenge. Further investigations exploring non-lethal responses in conjunction with the shear stress response of sensor cells and employing CFD under varying hydrodynamic stresses would provide valuable insights into this intricate relationship.

We utilized the average P/V as a representative hydrodynamic stress in stirred bioreactors and correlated it with the shear stress response of the sensor cells. This average P/V was estimated using a power number specific to the impellers employed in our experiments. Our assumption is that a higher average P/V induces more shear stress on sensor cells, and it is commonly employed for scale-up purposes. However, it is crucial to note that this average P/V alone may not comprehensively represent hydrodynamic stress. We acknowledge the significance of considering other parameters, such as the maximum P/V occurring in the vicinity of the impellers, and the ratio of this maximum P/V to the average P/V. Recent literature emphasizes the importance of adopting a multi-parameter approach when linking hydrodynamic and cellular effects (Pörtner et al., 2024). In fact, recent studies have indicated that the commonly used hydrodynamic parameter for scale up, average P/V, does not always suffice (Freiberger et al., 2022; Pörtner et al., 2024). For instance, Freiberger et al. conducted CFD simulations and CHO cell cultivation in two different bioreactors (one with a single impeller and the other with three impellers) at various agitation rates (Freiberger et al., 2022). They found that cells in the three-impeller bioreactor were successfully cultivated at much higher agitation rates due to its lower P/V max and consequently a lower ratio of P/V max to the average across a wide range of P/V. Considering this context, it is desirable to investigate our sensors in relation to other hydrodynamic stress parameters (*e.g.*, maximum P/V and the ratio of max to mean) in addition to average P/V to further validate our sensors. To achieve this, a comprehensive CFD analysis is necessary to obtain maximum P/V values for stirred bioreactors.

5. Conclusion

In this study, we developed the CHO-DG44 cell line-based shear stress sensor and tested it in commercial small-scale bioreactors. The stress-sensitive-promoter EGR-1 in the engineered CHO cells expresses GFP upon shear stress. Using chemically induced and fluidic shear stress, we confirmed stable expression of GFP by the sensor for more than a month and examined its sensitivity and operating range. Following this characterization, we evaluated the shear stress level of the commercial small-scale bioreactors under different vessel designs and operating conditions (stirring speed and duration). The sensor expressed more GFP in response to higher stress magnitude and exposure time under harsh agitation conditions. No shear stress response was observed under typical bioprocess conditions at less than 1000 rpm agitation. Further improvement of the sensor in terms of time response, dynamic range, and sensitivity could facilitate the design of various bioreactor vessels with a low shear stress profile, which could be beneficial for shear sensitive cell lines for bioprocessing.

CRediT authorship contribution statement

Samin Akbari: Conceptualization, Methodology, Supervision, Validation, Writing – original draft. **Christoph Zehe:** Supervision, Writing – review & editing. **Ann-Cathrin Leroux:** Formal analysis, Investigation, Methodology, Validation, Visualization, Writing – original draft. **Taehong Kwon:** Formal analysis, Investigation, Methodology, Validation, Visualization, Writing – original draft. **David Pollard:** Supervision, Writing – review & editing. **Han Zang:** Writing – review & editing, Formal analysis, Investigation, Methodology, Validation.

Declaration of Competing Interest

The authors declare the following financial interests/personal relationships which may be considered as potential competing interests: Taehong Kwon, Ann-Cathrin Leroux, David Pollard, Christoph Zehe, and Samin Akbari have patent applications currently pending with respect to

topics in this article.

Data availability

Data will be made available on request.

Acknowledgement

This work was internally funded by Sartorius Stedim North America, United States, and Sartorius Stedim Cellca GmbH, Germany.

Conflict of interest statement

T.K., A.-C.L., D.P., C.Z., and S.A. have patent applications currently pending with respect to topics in this article.

Appendix A. Supporting information

Supplementary data associated with this article can be found in the online version at doi:10.1016/j.jbiotec.2024.04.016.

References

Bender, E., 2021. Stem-cell start-ups seek to crack the mass-production problem. Nature 597, S20–S21.
Chalmers, J.J., 2015. Mixing, aeration and cell damage, 30+ years later: what we learned, how it affected the cell culture industry and what we would like to know more about. Curr. Opin. Chem. Eng. 10, 94–102.
Chiu, J.-J., Chen, L.-J., Lee, P.-L., Lee, C.-I., Lo, L.-W., Usami, S., Chien, S., 2003. Shear stress inhibits adhesion molecule expression in vascular endothelial cells induced by coculture with smooth muscle cells. Blood 101, 2667–2674.
Davies, S.L., Lovelady, C.S., Grainger, R.K., Racher, A.J., Young, R.J., James, D.C., 2013. Functional heterogeneity and heritability in CHO cell populations. Biotechnol. Bioeng. 110, 260–274.
Ding, N., Li, C., Guo, M., Mohsin, A., Zhang, S., 2019. Numerical simulation of scaling-up an inverted frusto-conical shaking bioreactor with low shear stress for mammalian cell suspension culture. Cytotechnology 71, 671–678.
Dong, J., Gu, Y., Li, C., Wang, C., Feng, Z., Qiu, R., Chen, B., Li, J., Zhang, S., Wang, Z., Zhang, J., 2009. Response of mesenchymal stem cells to shear stress in tissue-engineered vascular grafts. Acta Pharmacol. Sin. 30, 530–536.
Fallon, M.E., Mathews, R., Hinds, M.T., 2022. In vitro flow chamber design for the study of endothelial cell (patho)physiology. J. Biomech. Eng. 144, 020801. https://asmedigitalcollection.asme.org/biomechanical/article/144/2/020801/1114550/In-Vitro-Flow-Chamber-Design-for-the-Study-of.
Freiberger, F., Budde, J., Ateş, E., Schlüter, M., Pörtner, R., Möller, J., 2022. New insights from locally resolved hydrodynamics in stirred cell culture reactors. Processes 10, 107.
Gareau, T., Lara, G.G., Shepherd, R.D., Krawetz, R., Rancourt, D.E., Rinker, K.D., Kallos, M.S., 2014. Shear stress influences the pluripotency of murine embryonic stem cells in stirred suspension bioreactors. J. Tissue Eng. Regen. Med. 8, 268–278.
Guyot, Y., Luyten, F., Schrooten, J., Papantoniou, I., Geris, L., 2015. A three-dimensional computational fluid dynamics model of shear stress distribution during neotissue growth in a perfusion bioreactor. Biotechnol. Bioeng. 112, 2591–2600.
Hu, W., Berdugo, C., Chalmers, J.J., 2011. The potential of hydrodynamic damage to animal cells of industrial relevance: current understanding. Cytotechnology 63, 445–460.
Huang, Y., Chen, X., Che, J., Zhan, Q., Ji, J., Fan, Y., 2019. Shear stress promotes arterial endothelium-oriented differentiation of mouse-induced pluripotent stem cells. Stem Cells Int. 2019, 1–13. https://www.hindawi.com/journals/sci/2019/1847098/.
Huang, Y., Qian, J.-Y., Cheng, H., Li, X.-M., 2021. Effects of shear stress on differentiation of stem cells into endothelial cells. WJSC 13, 894–913.
ibidi GmbH. 2022. Application Note 11: Shear Stress and Shear Rates for ibidi µ-Slides Based on Numerical Calculations. Application Note. ibidi GmbH. https://ibidi.com/img/cms/support/AN/AN11_Shear_stress.pdf.
Jackson, M.L., Bond, A.R., George, S.J., 2023. Mechanobiology of the endothelium in vascular health and disease: in vitro shear stress models. Cardiovasc Drugs Ther. 37, 997–1010.
Julaey, M., Hosseini, M., Amani, H., 2016. Stem cells culture bioreactor fluid flow, shear stress and microcarriers dispersion analysis using computational fluid dynamics. J. Appl. Biotechnol. Rep. 3, 425–431. https://www.biotechrep.ir/article_69217.html.
Kamen, A.A., Chavarie, C., André, G., Archambault, J., 1992. Design parameters and performance of a surface baffled helical ribbon impeller bioreactor for the culture of shear sensitive cells. Chem. Eng. Sci. 47, 2375–2380.
Kepp, O., Galluzzi, L., Lipinski, M., Yuan, J., Kroemer, G., 2011. Cell death assays for drug discovery. Nat. Rev. Drug Discov. 10, 221–237.
McCormick, S.M., Frye, S.R., Eskin, S.G., Teng, C.L., Lu, C.-M., Russell, C.G., Chittur, K. K., McIntire, L.V., 2003. Microarray analysis of shear stressed endothelial cells. Biorheology 40, 5–11. https://content.iospress.com/articles/biorheology/bir159.
Nsiah, B.A., Ahsan, T., Griffiths, S., Cooke, M., Nerem, R.M., McDevitt, T.C., 2014. Fluid shear stress pre-conditioning promotes endothelial morphogenesis of embryonic stem cells within embryoid bodies. Tissue Eng. Part A 20, 954–965.
Okahara, K., Kambayashi, J., Ohnishi, T., Fujiwara, Y., Kawasaki, T., Monden, M., 1995. Shear stress induces expression of CNP gene in human endothelial cells. FEBS Lett. 373, 108–110.
Petralia, S., Conoci, S., 2017. PCR technologies for point of care testing: progress and perspectives. ACS Sens. 2, 876–891.
Polizzi, K.M., 2022. Biosensors of the well-being of cell cultures. In: Thouand, G. (Ed.), Handbook of Cell Biosensors. Springer International Publishing, Cham, pp. 71–88. https://link.springer.com/referenceworkentry/10.1007/978-3-030-23217-7_119.
Polizzi, K.M., Kontoravdi, C., 2015. Genetically-encoded biosensors for monitoring cellular stress in bioprocessing. Curr. Opin. Biotechnol. 31, 50–56. https://www.sciencedirect.com/science/article/abs/pii/S0958166914001396.
Pörtner R., Freiberger F., Möller J. 2024. Review on the Impact of Impeller-induced Hydrodynamics on Suspension Cell Culture for Production of Biopharmaceuticals. Chemie Ingenieur Technik:cite.202300162. https://onlinelibrary.wiley.com/doi/full/10.1002/cite.202300162.
Riehl B.D., Donahue H.J., Lim J.Y. 2017. Fluid Flow Control of Stem Cells With Investigation of Mechanotransduction Pathways. In:. Biology and Engineering of Stem Cell Niches. Elsevier, pp. 257–272. https://www.sciencedirect.com/science/article/abs/pii/B9780128027349000172.
Rotondi, M., Grace, N., Betts, J., Bargh, N., Costariol, E., Zoro, B., Hewitt, C.J., Nienow, A.W., Rafiq, Q.A., 2021. Design and development of a new ambr250® bioreactor vessel for improved cell and gene therapy applications. Biotechnol. Lett. 43, 1103–1116.
Sartorius Stedim Biotech. 2020. ambr® 250 modular Operator Manual. Sartorius Stedim Biotech.
Seefried, L., Mueller-Deubert, S., Schwarz, T., Lind, T., Mentrup, B., Kober, M., Docheva, D., Liedert, A., Kassem, M., Ignatius, A., others, 2010. A small scale cell culture system to analyze mechanobiology using reporter gene constructs and polyurethane dishes. Eur. Cells Mater. 20, 344–355. https://www.ecmjournal.org/papers/vol020/vol020a28.php.
Shiragami, N., Unno, H., 1994. Effect of shear stress on activity of cellular enzyme in animal cell. Bioprocess Eng. 10, 43–45. https://link.springer.com/article/10.1007/BF00373534.
Stoddart, M.J., 2011. Cell viability assays: introduction. In: Stoddart, M.J. (Ed.), Methods and Protocols: Methods and Protocols. Humana Press, Totowa, NJ, pp. 1–6. https://doi.org/10.1007/978-1-61779-108-6_1.
Traub, O., Berk, B.C., 1998. Laminar shear stress. Arterioscler. Thromb. Vasc. Biol. 18, 677–685. https://www.ahajournals.org/doi/10.1161/01.atv.18.5.677?url_ver=Z39.88-2003&rfr_id=ori:rid:crossref.org&rfr_dat=cr_pub%20%200pubmed.
Varma, S., Fendyur, A., Box, A., Voldman, J., 2017. Multiplexed cell-based sensors for assessing the impact of engineered systems and methods on cell health. Anal. Chem. 89, 4663–4670.
Varma, S., Voldman, J., 2015. A cell-based sensor of fluid shear stress for microfluidics. Lab Chip 15, 1563–1573. https://pubs.rsc.org/en/content/articlelanding/2015/lc/c4lc01369g.
Verma, R., Mehan, L., Kumar, R., Kumar, A., Srivastava, A., 2019. Computational fluid dynamic analysis of hydrodynamic shear stress generated by different impeller combinations in stirred bioreactor. Biochem. Eng. J. 151, 107312.
Wurm, M.J., Wurm, F.M., 2021. Naming CHO cells for bio-manufacturing: Genome plasticity and variant phenotypes of cell populations in bioreactors question the relevance of old names. Biotechnol. J. 16, 2100165. https://analyticalsciencejournals.onlinelibrary.wiley.com/doi/10.1002/biot.202100165.
Xiao, L., Wang, G., Jiang, T., Tang, C., Wu, X., Sun, T., 2011. Effects of shear stress on the number and function of endothelial progenitor cells adhered to specific matrices. JABB 9, 193–198. https://journals.sagepub.com/doi/10.5301/JABB.2011.6475.
Young, A., Wu, W., Sun, W., Larman, H.B., Wang, N., Li, Y.-S., Shyy, J.Y., Chien, S., García-Cardeña, G., 2009. Flow activation of AMP-activated protein kinase in vascular endothelium leads to krüppel-like factor 2 expression. Arterioscler. Thromb., Vasc. Biol. 29, 1902–1908. https://www.ahajournals.org/doi/10.1161/ATVBAHA.109.193540?url_ver=Z39.88-2003&rfr_id=ori:rid:crossref.org&rfr_dat=cr_pub%20%200pubmed.
Zeh, N., Bräuer, M., Raab, N., Handrick, R., Otte, K., 2022. Exploring synthetic biology for the development of a sensor cell line for automated bioprocess control. Sci. Rep. 12, 2268. https://www.nature.com/articles/s41598-022-06272-x.
Zhang, Y., Dong, Y.-H., Liao, B., Nie, Y.-M., Wan, J., Xiong, L.-L., Fu, Y., Xie, X.-J., Yu, F.-X., 2019. Shear stress regulates eNOS signaling in human umbilical vein endothelial cells via SRB1-PI3KAP1 pathway. fmcp 16. https://www.openaccessjournals.com/articles/shear-stress-regulates-enos-signaling-in-human-umbilical-vein-endothelial-cells-via-srb1pi3kap1-pathway-12980.html.